Computers and Concrete, *Vol. 11, No. 5 (2013) 441-462*
DOI: http://dx.doi.org/10.12989/cac.2013.11.5.441

A new method solving the temperature field of concrete around cooling pipes

Zhenyang Zhu*[1], Sheng Qiang[2] and Weimin Chen[1]

[1]Hydrochina Huadong Engineering Corporation, Hangzhou 310014, PR China
[2]College of Water conservancy & Hydropower Engineering, Hohai University, Nanjing 210098, PR China

(Received February 14, 2011, Revised February 22, 2012, Accepted October 30, 2012)

Abstract. When using the conventional finite element method, a great number of grid nodes are necessary to describe the large and uneven temperature gradients in the concrete around cooling pipes when calculating the temperature field of mass concrete with cooling pipes. In this paper, the temperature gradient properties of the concrete around a pipe were studied. A new calculation method was developed based on these properties and an explicit iterative algorithm. With a small number of grid nodes, both the temperature distribution along the cooling pipe and the temperature field of the concrete around the water pipe can be correctly calculated with this new method. In conventional computing models, the cooling pipes are regarded as the third boundary condition when solving a model of concrete with plastic pipes, which is an approximate way. At the same time, the corresponding parameters have to be got by expensive experiments and inversion. But in the proposed method, the boundary condition is described strictly, and thus is more reliable and economical. And numerical examples were used to illustrate that this method is accurate, efficient and applicable to the actual engineering.

Keywords: calculation method; temperature field; mass concrete; cooling pipes; boundary condition

1. Introduction

Pipe cooling has been an effective measure to prevent concrete from cracking (Xie *et al.* 2005, Wang *et al.* 2008). Nowadays, pipe cooling are widely used in walls of nuclear power plants (Dundulis *et al.* 2007, Silin *et al.* 2010), and in civil building concrete walls for air-conditioning or other purposes (Koschenz *et al.* 1999, Tan *et al.* 2010, He *et al.* 2010, Ni *et al.* 2011).

However, calculating the temperature field of mass concrete with cooling pipes using an available and reliable method is a rather difficult problem due to the large and uneven temperature gradients of the concrete around pipes. The temperature of fresh concrete is especially hard to simulate because of hydration heat. 3D (three-dimensional) finite element method is a powerful measure to solve this problem, and has been studied for a long time. Early studies, such as pseudo 3D and 3D finite element methods, were developed and used for a long time (Kawaraba *et al.* 1986, Machida *et al.* 1987).

However, the pseudo 3D method was converted from a simple two-dimensional (2D) analysis method and cannot correctly apply boundary conditions for the atmosphere and cooling water

*Corresponding author, Ph.D., E-mail: 1219921552@qq.com

http://www.techno-press.org/?journal=cac&subpage=8 ISSN: 1598-8198 (Print), 1598-818X (Online)

convection. The equivalent heat methods (Zhu 2003) has widely been applied in mass concrete structures such as concrete dams and got satisfying results. But it does not consider the temperature distribution of the concrete near pipes. It is important in the walled structure.

Then, some calculation methods based on heat transfer by heat balance principle is developed, such as Jin Keun Kim method (Kim *et al.* 2001). The water temperature distribution along the pipe can be calculated using these methods, and the boundary conditions of the atmosphere can also be applied. However, the temperature gradient properties are simplified. Thus, the calculation result is sometimes unreliable, or a great number of grid nodes have to be used to guarantee accuracy. Also based on the heat balance principle, an explicit iterative algorithm was developed by former researchers (Zhu *et al.* 2003, Zhu 2010). With the development of the corresponding technique to find the pipe boundary along the pipe line, this method is also suitable for practical problems with numerous snake-shaped internal cooling pipes (Deng *et al.* 2008). This method involves a strict mathematical deduction, but it also requires a large number of grid nodes to ensure the accuracy of temperature gradients in the concrete surrounding the pipe.

Given the temperature gradient properties of the concrete near the pipe, a calculation method for temperature field around pipe was developed in this paper based on the explicit iterative algorithm method. With a relatively small number of grid nodes, both the temperature distribution along the cooling pipe and the temperature field of the concrete around the water pipe can be correctly calculated by this new method. And numerical examples were used to illustrate that this method is accurate, efficient and applicable to the actual engineering in this paper.

2. Fundamental theories

2.1 Fourier's law of heat conduction

Assume that the material obeys Fourier's law of heat conduction

$$\frac{\partial T}{\partial t} = a\left(\frac{\partial^2 T}{\partial x^2} + \frac{\partial^2 T}{\partial y^2} + \frac{\partial^2 T}{\partial z^2}\right) + \frac{\partial \theta}{\partial \tau} \qquad \left(\forall (x,y,z) \in R\right) \tag{1}$$

where T is the temperature, α is the thermal diffusivity, θ is the adiabatic temperature rise, t and τ stand for the time and age, respectively, and R is the domain studied.

2.2 Formulas for adiabatic temperature rise

There are several different formulas for adiabatic temperature rise, or the rate of adiabatic temperature rise (Schutter 2002, Zhang *et al.* 2002, Zhu 2003). And there are also some experiment and back analysis about the adiabatic temperature rise (Wang *et al.* 2008).

Zhu (2003) considered that rate of adiabatic temperature rise can be expressed by

$$\frac{d\left(\theta_a(\tau)\right)}{dt} = \theta_0\, ab\tau^{b-1}e^{-a\tau^b} \tag{2}$$

where θ_0 is the maximum adiabatic temperature rise of the concrete, τ is the age of the concrete.

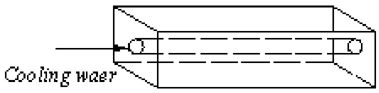

Fig. 1 Sketch of pipe cooling in concrete

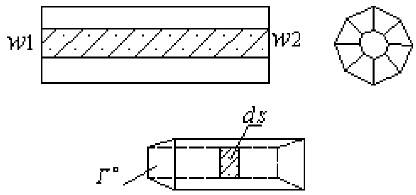

Fig. 2 Heat exchange faces

Schutter (2002) considered that the rate of temperature increase in fresh concrete can be described as

$$\frac{d(\theta_a(\tau))}{dt} = c[\sin(\pi\alpha)]^a \exp(-b\alpha) \tag{3}$$

where α is the degree of hydration.

2.3 Calculation of the temperature field based on the explicit algorithm

The deduction of the calculation of the temperature field based on the explicit algorithm can be shown as following:

Fig. 1 is a section of pipe in concrete, and Fig. 2 is the heat exchange face.

By studying the heat exchange between water and concrete, the heat transfer through the pipe surface within time *dt* can be expressed as

$$dQ_c = \iint_{\Gamma^0} q_i ds\ dt = -\lambda \iint_{\Gamma^0} \frac{\partial T}{\partial n} ds\ dt \tag{4}$$

where λ is the thermal conductivity of the concrete, Γ^0 is the interface between the concrete and pipe, and n is the interface normal vector.

The heat absorbed by water flowing through the section of pipe within time *dt* is

$$dQ_1 = c_w \rho_w \Delta T_w q_w dt \tag{5}$$

where c_w, ρ_w and q_w stand for the specific heat, density of water and flux, respectively, and ΔT_w is the water temperature difference between the inlet and outlet of the pipe section.

Given that the volume of the pipe is very small, and the water body heat increment in the pipe section can be neglected. From Eqs. (4) and (5), the water temperature increment within the pipe section can be found

$$\Delta T_{wi} = \frac{-\lambda}{c_w \rho_w q_w} \iint_{\Gamma^0} \frac{\partial T}{\partial n} ds \tag{6}$$

Because the inlet water temperature is known, the water temperature at any pipe section along the pipe can be calculated step by step. If there is a water pipe divided into several pipe sections and the water temperature increment of one pipe section is ΔT_{wj} and the inlet water temperature is T_{w0}, then

$$T_{wi} = T_{w0} + \sum_{j=1}^{i} \Delta T_{wj} \tag{7}$$

Because the unknown temperature gradient on the interface between the concrete and pipe affects the water temperature distribution along the pipe, it is a non-linearity problem of the boundary conditions and cannot be solved directly. Therefore, an iterative method should be used.

For the first iteration, the water temperature along water pipe is assumed equal to the inlet water temperature. The approximate solution of the temperature field can be calculated with Eq. (1). Then, the water temperature distribution along the water pipe can be calculated with Eqs. (6) and (7). The process is then repeated until the water temperature distribution along the water pipe and the concrete temperature field reaches a steady-state solution.

2.4 Basic theories of boundary conditions

There are four kinds of boundary conditions according to the way heat exchanges.

(1) The first boundary condition:

Surface temperature of concrete is known as function of time, which can be expressed by

$$T(\tau) = f(\tau) \tag{8}$$

where T is temperature of concrete surface and τ is time.

(2) The second boundary condition

Heat flux of concrete surface is known as function of time, which can be expressed by

$$-\lambda \frac{\partial T}{\partial n} = f(\tau) \tag{9}$$

where n is the concrete surface normal vector, λ is the thermal conductivity of the concrete.

(3) The third boundary condition

When contacted with air, heat flux of concrete surface can be expressed by

$$q = -\lambda \frac{\partial T}{\partial n} \tag{10}$$

Under the third boundary condition, it is supposed that heat flux of concrete surface is proportional to the temperature difference between air temperature and surface temperature of concrete, and can be expressed by

$$-\lambda \frac{\partial T}{\partial n} = \beta(T - T_a) \tag{11}$$

where T_a is the air temperature and β is heat transfer coefficient.

(4) The forth boundary condition

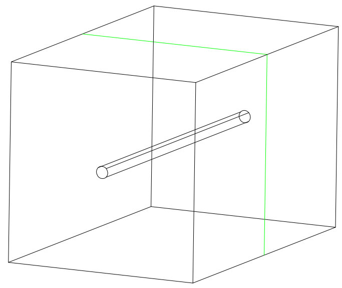

Fig. 3 Mass concrete with cooling pipe

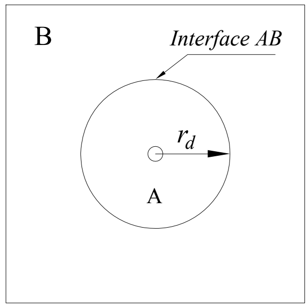

Fig. 4 Typical cross-section of Fig. 3

When two materials contact well, the temperatures of their interface and heat flux is continuous which can be expressed by

$$\begin{cases} T_1 = T_2 \\ \lambda_1 \dfrac{\partial T}{\partial n} = \lambda_2 \dfrac{\partial T}{\partial n} \end{cases} \tag{12}$$

where T_1 and T_2 are the interface temperature of two materials, λ_1 and λ_2 are the thermal conductivities of two materials.

When using metal pipes, temperature difference between inner surface and outer surface can be neglected. For plastic pipes, temperature difference between inner surface and outer surface should be taken into consideration. Inner surface of the pipe should be regarded as the first boundary condition, while the interface between concrete and pipe should be regarded as the fourth boundary condition.

3. Calculation method of temperature field around water pipe

3.1 Temperature characteristics of the concrete around a pipe

Because the heat convection coefficient between the water and the pipe is much greater than that between the concrete and the air, a region is found around the pipe where the temperature gradient is perpendicular to the pipe surface. The range of the region is highly relevant to the thickness. Generally, compared with a thin-wall structure made of high-hydration heat concrete, the range of the region in mass concrete made of low-hydration heat concrete is much greater. According to whether the temperature gradient is perpendicular to the pipe surface, the mass concrete with cooling pipes can be separated into two parts: part A is the circle area with a radius r_d where the temperature gradient is perpendicular to the pipe surface, and part B is the rest (shown in Figs. 3-5). Theoretically, r_d can be greater than 0.12 m for almost all structures and situations and even can be greater than 0.25 m for some structures and situations, but r_d is recommended to be 0.1 m to satisfy all situations (The value of r_d is proved in numerical example 1).

In Fig. 5(a), r_a is the outer radius of the pipe. Assuming that there is a circular-arc surface with angle φ and that the distance from the center of the pipe to the circular-arc surface is r_x (shown in

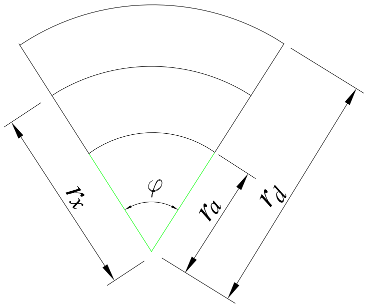

(a) Sectional drawing with angle φ

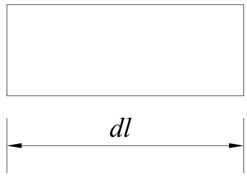

(b) Length of a section of pipe

Fig. 5 One typical segment of part A

Fig. 5(a)). The heat transferred through the circular-arc surface within time $d\tau$ is

$$Q_4 = Q_1 + Q_2 - Q_3 \tag{13}$$

where Q_1 is the heat transfer through the interface AB (shown in Fig. 4) within time $d\tau$, Q_2 is the heat caused by the hydration of the concrete between r_x and r_d within time $d\tau$, and Q_3 is the heat stored in the concrete between r_x and r_d within time $d\tau$, Q_4 is the heat transferred through the circular-arc surface within time $d\tau$.

The heat caused by the hydration of the concrete between r_x and r_d within time $d\tau$ is

$$Q_2 = \frac{\varphi\left(r_d^2 - r_x^2\right)\Delta\theta_a c_c \rho_c dl}{2} \tag{14}$$

where $\Delta\theta_a$ is the adiabatic temperature rise which can be expressed by formulas such as Eqs. (2) and (3) , dl is the length of the pipe section, c_c is the specific heat of the concrete, and ρ_c is the density of the concrete.

The heat stored in the concrete between r_x and r_d within time $d\tau$ is

$$Q_3 = \frac{\varphi\left(r_d^2 - r_x^2\right)\Delta\theta_b c_c \rho_c dl}{2} \tag{15}$$

where $\Delta\theta_b$ is the temperature increment in part A within time $d\tau$.

Then according to Eqs. (13)-(15),the heat transferred through the circular-arc surface within time $d\tau$(Q_4) can be expressed by

$$Q_4 = Q_1 + \frac{\varphi\left(r_d^2 - r_x^2\right)\left(\Delta\theta_a - \Delta\theta_b\right)c_c \rho_c dl}{2} \tag{16}$$

Define N_x as the temperature gradient on the circular-arc surface, then Q_4 can also expressed by

$$Q_4 = N_x \lambda \varphi\, r_x dl d\tau \tag{17}$$

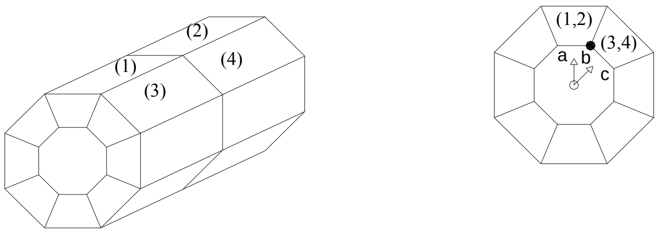

Fig. 6 Elements around the node

where λ is the thermal conductivity of the concrete.
Using Eqs. (16) and (17)

$$N_x = \frac{2Q_1 + \varphi \left(r_d^2 - r_x^2\right)\left(\Delta\theta_a - \Delta\theta_b\right)c_c\rho_c dl}{2\lambda\varphi\, r_x dl\, d\tau} \tag{18}$$

3.2 Simulation of the temperature field in part A when using a metal pipe

The interface PC is defined as the interface between the pipe and concrete. Because the temperature gradient in part A can be fitted by Eq. (18), within an angle φ (shown in Fig. 5(a)) the temperature difference between the interface AB (shown in Fig. 4) and interface PC is

$$\Delta T_{i1} = \int_{r_a}^{r_d} \frac{2Q_1 + \varphi \left(r_d^2 - r_x^2\right)\left(\Delta\theta_a - \Delta\theta_b\right)c_c\rho_c dl}{2\lambda\varphi\, r_x dl\, d\tau} dr_x \tag{19}$$

There is a node belonging to four elements (#1, #2, #3 and #4 element in Fig. 6). Surface ab is part of interface AB, which belongs to elements #1 and #2, and surface bc is also part of interface AB, belonging to elements #3 and #4.

Eq. (19) gives the temperature difference between the interface PC and the interface AB on the four elements, and they are denoted as ΔT_{ab1}, ΔT_{ab2}, ΔT_{bc3} and ΔT_{bc4}. Then, the temperature difference between the interface PC and the node is

$$\Delta T_i = \frac{\Delta T_{ab1} + \Delta T_{ab2} + \Delta T_{bc3} + \Delta T_{bc4}}{4} \tag{20}$$

Based on the heat balance principle and the combination of Eqs. (14) and (15), the water temperature increment within the pipe section is

$$\Delta T_{wi} = \frac{-\lambda \iint\limits_{\Gamma^{AB}} \frac{\partial T}{\partial n} ds d\tau + Q_2 - Q_3}{c_w \rho_w q_w d\tau} \tag{21}$$

where Γ^{AB} is the interface AB.

Based on Eqs. (14), (15) and (21) and the number of the elements around the pipe is m

$$\Delta T_{wi} = \frac{-2\lambda \iint_{\Gamma^{AB}} \frac{\partial T}{\partial n} ds d\tau + \sum_{k=1}^{m} \left[\varphi_k c_c \rho_c \left(r_d^2 - r_a^2 \right) \left(\Delta\theta_a - \Delta\theta_b \right) dl_i \right]}{2 c_w \rho_w q_w d\tau} \tag{22}$$

where $\sum_{k=1}^{m}(\varphi_k) = 2\pi$ and dl_i is the length of the pipe section.

When using a metal pipe, the temperature difference between the inner and outer surfaces of the pipe can be neglected. Thus, the temperature distribution on the interface AB along the pipe is

$$T_{si} = T_{w0} + \sum_{j=1}^{i} \Delta T_{wj} + \Delta T_i \tag{23}$$

where T_{w0} is the inlet water temperature.

$\Delta\theta_b$ can be calculated using the following method.

Without considering $\Delta\theta_b$, the temperature difference between the interface PC and the interface AB at time τ is ΔT_{i1}^{est}, without considering $\Delta\theta_b$, the water temperature increment in every pipe section at time τ is ΔT_{wi}^{est}, then, the average temperature in part A, within angle φ, is

$$T_{\tau}^{aver} = \left\{ T_{w0} + \sum_{j=1}^{i} \Delta T_{wj}^{est} + \frac{2}{\left(r_d^2 - r_a^2 \right)} \int_{r_a}^{r_d} \left[\frac{\Delta T_{i1}^{est}}{\ln\left(\frac{r_d}{r_a}\right)} \ln\left(\frac{r_x}{r_a}\right) r_x \right] dr_x \right\}_{\tau} \tag{24}$$

Then

$$\Delta\theta_b = T_{\tau+\mathrm{d}\tau}^{\mathrm{aver}} - T_{\tau}^{\mathrm{aver}} \tag{25}$$

According to Eq. (22), the unknown temperature gradient on the interface AB affects the water temperature distribution along the pipe. It is also a non-linear boundary condition problem and cannot be directly solved. Therefore, an iterative method should also be used.

For the first iteration, the temperature on interface AB is assumed to be equal to the inlet water temperature. The approximate solution of the temperature field is obtained by Eq. (1). Then, the node temperature on the interface AB is found with Eq. (19). The process is repeated until the temperature on the interface AB along the pipe and the concrete temperature field reaches a steady-state solution.

The inlet water temperature is lower than the temperature on the interface AB. Thus, before the first iteration, the assumed temperature on the interface AB is lower than the actual temperature. After first iteration, the calculated temperature gradient on the interface AB along the pipe is much greater than the actual one. According to Eqs. (22) and (23), after first iteration, the calculated temperature on the interface AB along pipe is much higher than the actual value. For the same reason, the calculated temperature on the interface AB along the pipe is much lower than the actual value after the second iteration. When the iteration time is an odd number, after iteration, the calculated temperature on the interface AB will be higher than the actual one. However, when the

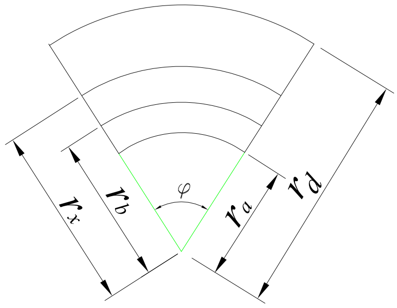

(a) Typical Sectional drawing

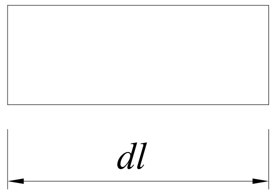

(b) Length of a section of pipe

Fig. 7 One typical segment of a plastic pipe and the surrounding concrete

iteration time is an even number, after iteration, the calculated value of temperature on the interface AB will be lower than the actual one.

When iteration time is N-1, the calculated temperature on the interface AB along the pipe is $\{T_s\}_{n-1}$, and when iteration time is N and the calculated temperature on the interface AB along the pipe is $\{T_s\}_n$. Compared with using $\{T_s\}_n$ as the water temperature distribution on the interface AB before N+1 iterations, using $\frac{1}{2}\left(\{T_s\}_{n-1}+\{T_s\}_n\right)$ greatly reduces the iteration number.

3.3 Simulation of the temperature field in part A when using a plastic pipe

When simulating the temperature field with metal pipes, the temperature difference between the inner and outer surface of the pipe can be neglected. However, for plastic pipes, it cannot be neglected.

Fig. 7 is a typical cross-section for the concrete around a plastic pipe. Define r_a and r_b as the radius of the pipe at the inner surface and outer surface. On a circular-arc surface with an angle φ and a distance from the center of the pipe to the circular-arc surface r_x, the temperature gradient can be expressed as

$$N_x = \begin{cases} N_a \dfrac{r_a}{r_x} & r_a \le r_x < r_b \\ \dfrac{2Q_1 + \varphi\left(r_d^2 - r_x^2\right)\left(\Delta\theta_a - \Delta\theta_b\right)c_c\rho_c dl}{2\lambda_2\varphi\, r_x dl\, d\tau} & r_b < r_x \le r_d \end{cases} \tag{26}$$

where N_a is the temperature gradient on inner surface of the pipe, λ_2 is the thermal conductivity of the concrete.

Define N_b as the temperature gradient of the concrete at the interface between the pipe and concrete.

Let $l_b=\varphi r_b$, and define λ_1 as the thermal conductivity of the pipe. Then, the heat transfer through the interface between the pipe and concrete within time $d\tau$ is

$$Q_p = \frac{N_a r_a \lambda_1 l_b dl d\tau}{r_b} \tag{27}$$

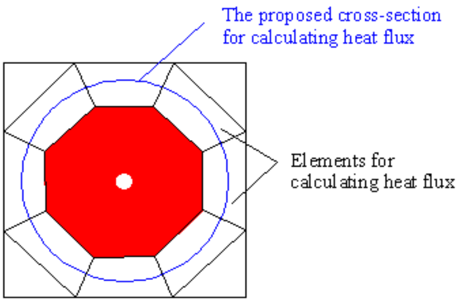

Fig. 8 The proposed cross-section for calculating heat flux

The heat transfer through the interface between the pipe and concrete within time $d\tau$ is

$$Q_c = N_b \lambda_2 l_b dl d\tau \tag{28}$$

It is obviously that $Q_p = Q_c$, and thus,

$$N_a = N_b \frac{\lambda_2 r_b}{\lambda_1 r_a} \tag{29}$$

Using Eqs. (18) and (29)

$$N_x = \begin{cases} N_b \dfrac{\lambda_2 r_b}{\lambda_1 r_x} & r_a \le r_x < r_b \\ \dfrac{2Q_1 + \varphi\left(r_d^2 - r_x^2\right)\left(\Delta\theta_a - \Delta\theta_b\right)c_c\rho_c dl}{2\lambda_2 \varphi\, r_x dl\, d\tau} & r_b < r_x \le r_d \end{cases} \tag{30}$$

where $N_b = \dfrac{2Q_1 + \varphi\left(r_d^2 - r_b^2\right)\left(\Delta\theta_a - \Delta\theta_b\right)c_c\rho_c dl}{2\lambda_2 \varphi\, r_b dl\, d\tau}$.

From Eq. (30), the temperature difference between interface AB and water is

$$\Delta T_{i1} = \int_{r_a}^{r_d} N_x dx \tag{31}$$

From Eqs. (1), (22), (23), (24), (25) and (31), the temperature field of the mass concrete with a plastic pipe can be calculated.

3.4 Requirements of elements for calculating heat flux

With this method, the element surrounding part A is used for calculating heat flux, and for those elements, the best value of the element size along the direction perpendicular to the surface of the pipe is 0.05 m. Except those elements, the value of the element size along the direction perpendicular to the surface of the pipe can be more than 0.5 m or even 1m, depending on the distance to the surface of the pipe.

When calculating heat flux by equations of this paper, using the blue cross-section shown in

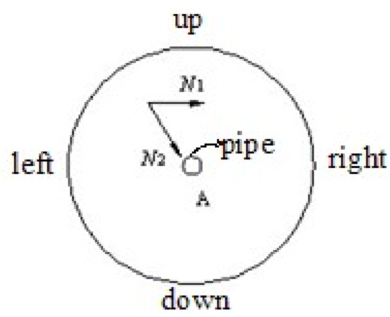

Fig. 9 Temperature gradient of concrete near water pipes

Fig. 8 (the red area refers to part A) can be more precise than using the interface between part A and part B.

4. Numerical and engineering examples

There are four numerical examples to illustrate that using this method to solve the temperature field around the cooling pipe.

4.1 Numerical example 1

Fig. 9 is a cross-section same as Fig. 4. If temperature gradient of the concrete near pipe is separated into two vectors shown in Fig. 9, then vector N_2 can be regarded as the vector caused by temperature difference between water and concrete, and N_1 can be regarded as the vector caused by temperature difference between left side and right side (or between upside and downside) of the concrete which has not taken into consideration in Eq. (18). So the extreme case should be a thin-wall structure with obvious temperature difference between two main sides.

In this example, the temperature gradient of a thin-wall structure with 15℃ temperature difference between two main sides is studied. Two cases are used to determinate the area where the temperature can be expressed by Eq. (18).
Case 1 is conventional FEM with lots of elements near pipe.
Case 2 is the proposed method.

4.1.1 Basic information

The length-width ratio of the thin-wall structure can be very large, and sometimes it may be only 0.5 m in width. Pipe cooling can effectively prevent such structures from cracking. The cooling pipes are usually arranged in the center of the wall, and the spacing between pipes is about 0.6 m along the height direction.

A mass concrete structure with the dimensions of 5.5 m×0.5 m×1.5 m (length×width×height) is used in this example. The rate of the adiabatic temperature rise is $d(\theta_a(\tau))/dt = 44.0\tau^{0.41}e^{-0.52\tau^{1.41}}$ (ºC/d).

The placement temperature is 30ºC. The air temperature of one side of the wall (one main side with a dimension of 5.5 m×1.5 m) is 15ºC, while other sides are 30ºC. The heat transfer

Table 1 Other thermal parameters

Position	Thermal conductivity (kJ/ (m^2•d•$^\circ$C))	Thermal diffusivity (m^2/h)	Specific heat (kJ/ kg•$^\circ$C)
Thin wall	228.48	0.079	1.10
Foundation	166.08	0.100	0.55

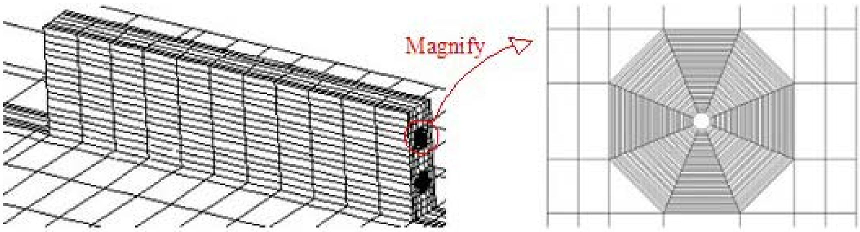

Fig. 10 Mesh for conventional FEM which need lots of node numbers

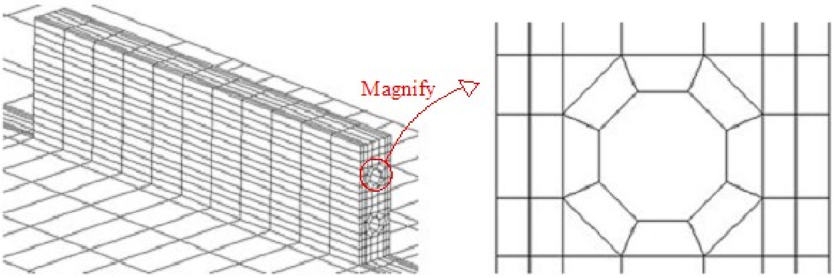

Fig. 11 The finite element mesh when using proposed method

coefficient between concrete and air is 42.5 kJ/ (m^2•h•ºC). Other thermal parameters are shown in Table 1. The inlet water temperature is 5ºC. Metal pipes are used in the two cases.

4.1.2 Mesh for conventional FEM method (case 1)

In order to simulate the temperature field near pipe precisely when using conventional FEM, the element size is 0.0045 m along the direction perpendicular to the surface of the pipe. The element mesh is shown in Fig. 10. The number of nodes for conventional FEM is 10784.

4.1.3 Mesh for proposed method (case 2)

When using proposed method, the concrete is separated into two parts. Temperature field of one part which is near water pipes is calculated by Eq. (18). The other part is calculated by FEM. When using proposed method, the part of temperature field calculated by Eq. (18) does not have influence on the efficiency of calculation.

(1) Mesh of the part calculated by FEM

Fig. 11 is the part of the element mesh used for FEM when using proposed method. The number of nodes in this model is 3296.

(2) The part of concrete near pipes

The temperature field of this part is calculated by Eq. (18), and does not have influence on

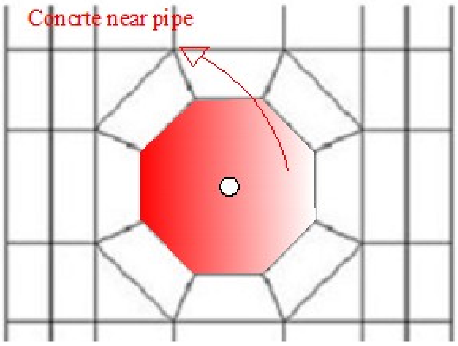

Fig. 12 The part of concrete near pipes

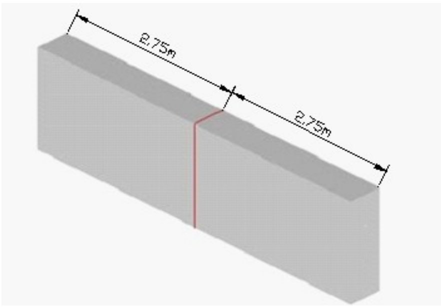

(a) Position of typical section

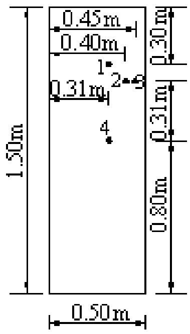

(b) Position of typical points

Fig. 13 Locations of typical section and typical points

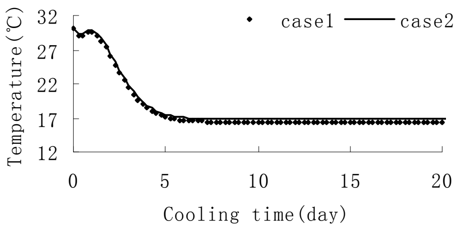

(a) Duration curve of point #1

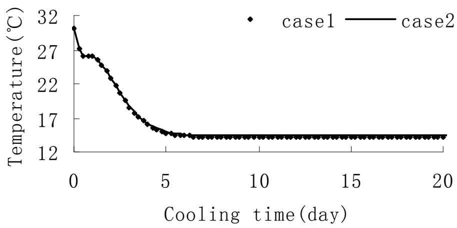

(b) Duration curve of point #2

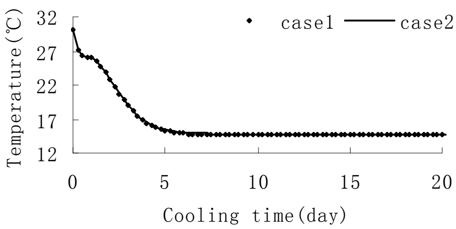

(c) Duration curve of point #3

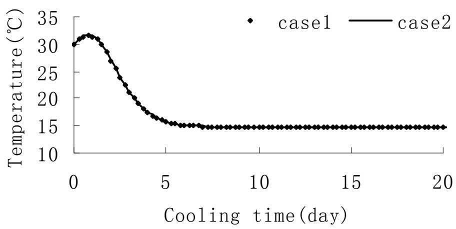

(d) Duration curve of point #4

Fig. 14 Temperature duration curves of typical points

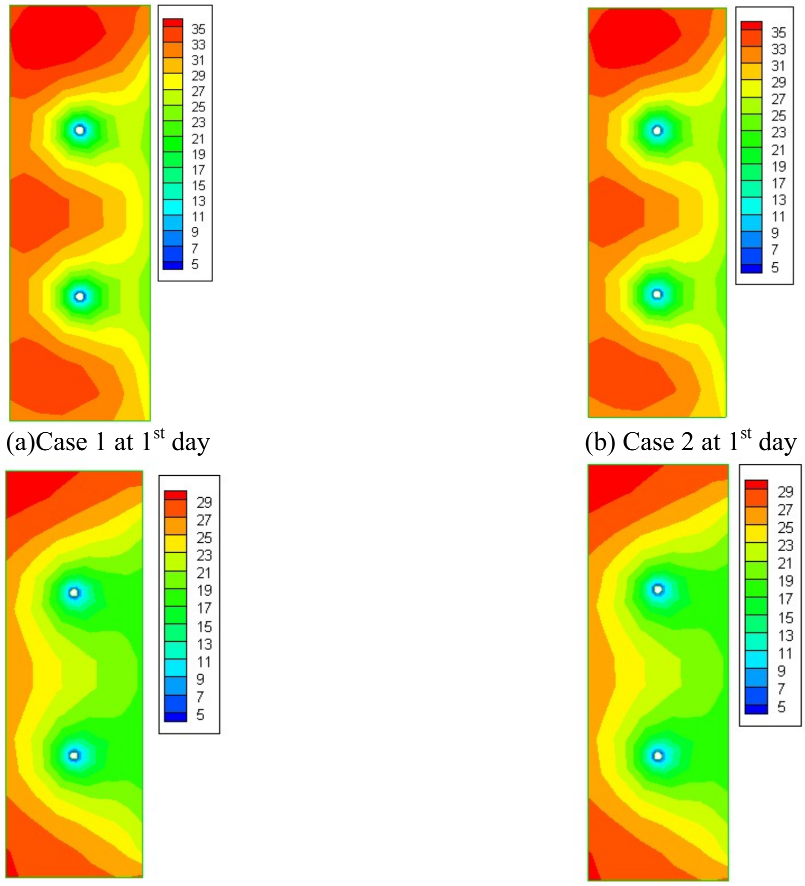

(a)Case 1 at 1st day (b) Case 2 at 1st day

(c) Case 1 at 3rd day (d) Case 2 at 3rd day

Fig. 15 Temperature distribution on a typical cross-section (°C)

efficiency of calculation. The radius of this part is 0.11 m (shown in Fig. 12).

4.1.4 Calculation results

(1)Typical section and typical points

Both typical section and typical points are shown in Fig. 13

(2)Analysis of temperature field

It is shown in Figs. 14 and 15 that the proposed method can precisely describe the temperature field near pipe using much fewer nodes than conventional FEM. It is also shown that temperature field of the area within 0.11m to the central of the pipe can be calculated by Eq. (18) for this extreme case.

Other cases show that structures with the much bigger width, such as concrete dams, the radius of the area can be expressed by Eq. (18) can even reach to 0.25 m.

4.2 Numerical example 2

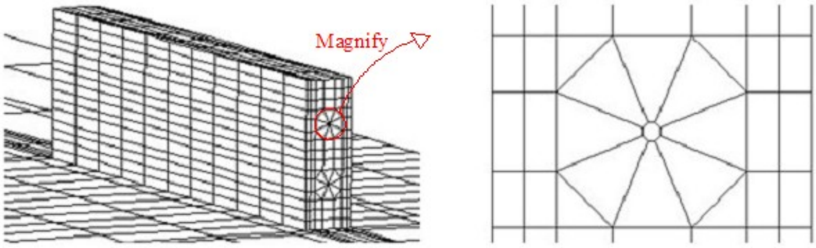

Fig. 16 Mesh for case 4 (use conventional FEM)

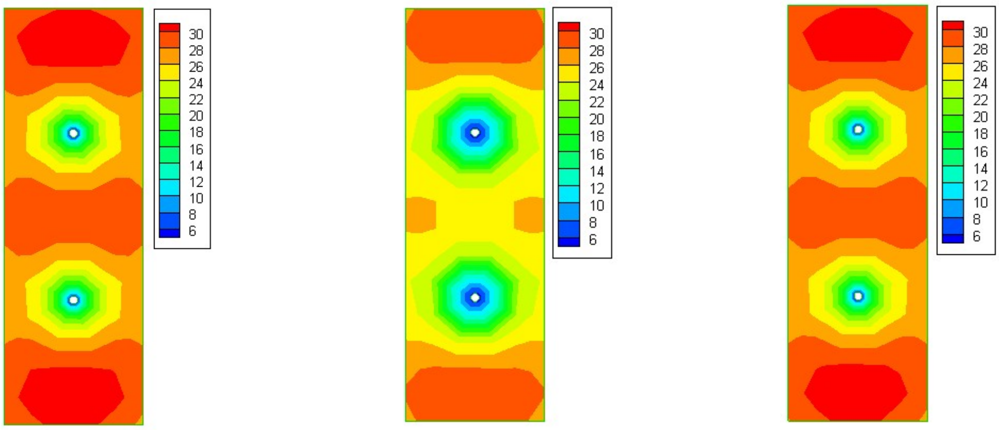

(a) Case 3 at 2nd day (b) Case 4 at 2nd day (c) Case 5 at 2nd day

Fig. 17 Typical section temperature distribution of three cases

In this numerical example, three cases are used to prove that the proposed method is much more precise than conventional FEM when the number of nodes is same.

Proposed method is used in case 3. In case 3 air temperatures of all sides of the wall is 25℃, and the other conditions in case 3 are same as case 2.

Conventional FEM is used in case 4 with the same number of node with case 3. The FEM mesh used for case 4 is shown in Fig. 16.

Conventional FEM is also used in case 5. In case 5 air temperatures of all sides of the wall is 25℃, the other conditions in case 5 are same as case 1. Both case 1 and case 5 use large number of element nodes to describe temperature field near pipes.

4.2.1 Analysis of typical section temperature distribution of three cases

Fig. 17 is the typical section temperature distribution of three cases. Compared with Figs. 17(a) and (b), it is shown that result calculated by proposed method is much different from conventional method with same number of nodes. Compared with Figs. 17(a) and (c), it is shown that the proposed method with much fewer number of nodes can achieve the same precision as the conventional FEM with huge number of nodes.

4.2.2 Analysis of temperature gradient

The temperature gradient distribution varies along different directions and at different cooling times. The temperature gradient distribution changes with different angle directions ω (shown in

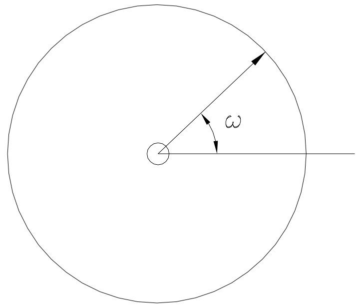

Fig. 18 The angle to study temperature field gradient in different direction

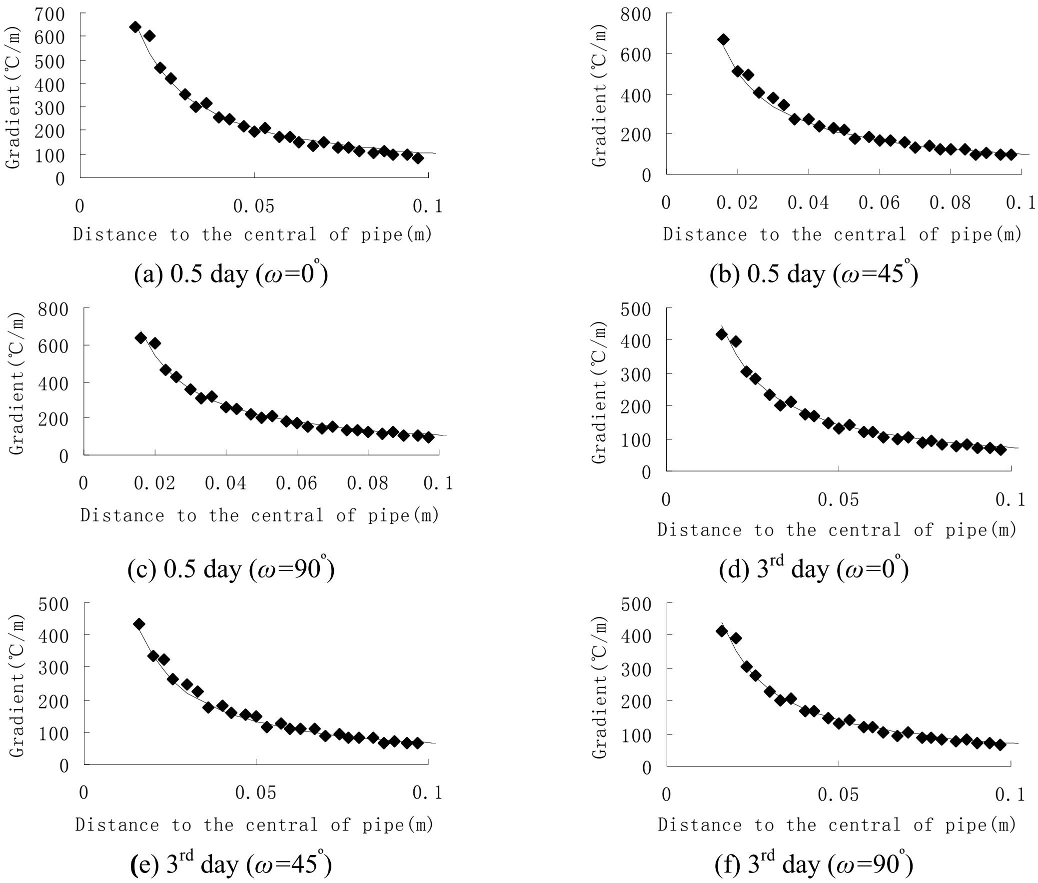

Fig. 19 Temperature gradient distribution of the concrete near pipe

Fig. 18)). For the pipe 1.05 m above the foundation, the temperature gradient distributions along the three different directions (ω=0º, 45º and 90º) and at three different cooling times (t=0.5d, 3.0d) are investigated. The calculation results are shown in Fig. 19.

As we all know, 8-node element can only describe the temperature field of the area where temperature gradient can be seen as a constant. It is shown in Fig. 19 that the temperature gradient of those concrete within 0.1 m to the center of the pipe cannot be seen as a constant unless huge element numbers are applied. Precise water temperature distribution is based on precise temperature gradient of the concrete near pipe so the proposed method can use much fewer nodes than conventional FEM to get precise temperature gradient of the concrete near pipe.

4.3 Numerical example 3

The pipe cross-section can be simplified to a square or octagon as long as the inner surface area of the pipe does not change after simplification. Compared with an octagonal pipe cross-section, the temperature of the concrete close to the pipe may be different when using a square pipe cross-section. However, for the concrete at a certain distance from the pipe, the temperature distribution is almost the same for both simplifications.

Properties of materials are same as example 1. The dimensions of model are shown in Fig. 23. The air temperature of all the sides is 30℃ except the right side of the typical cross-section with the air temperature of 15℃. Water temperature is 5℃.

There are also two cases to analyze the influence of pipe cross-section shape on the temperature field calculation results.

Case 6 is the conventional FEM with mesh shown in Fig. 20.

Case 7 is the proposed method with cross-section of the pipe simplified in to square. The concrete of this method is also separated into two parts which are shown in Figs. 21 and 22.

A typical cross-section and several typical points were chosen for a better analysis. The typical cross-section was same as in example 1, and the typical points were on the typical cross-section. The distances between points #1, #2 and #3 and the center of the pipe are 0.2 m, 0.58 m and 0.7 m (shown in Fig. 23).

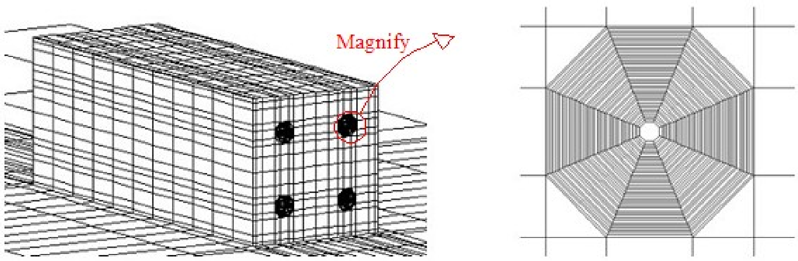

Fig. 20 Conventional FEM mesh

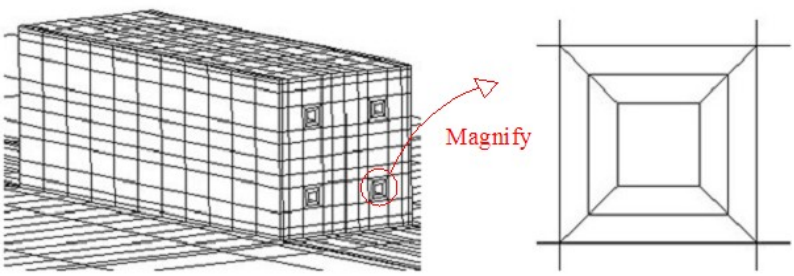

Fig. 21 The finite element mesh when using proposed method

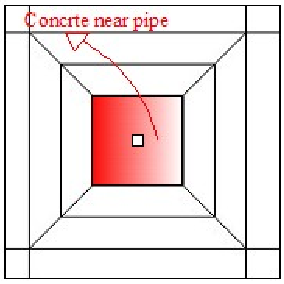

Fig. 22 The part of concrete near pipes

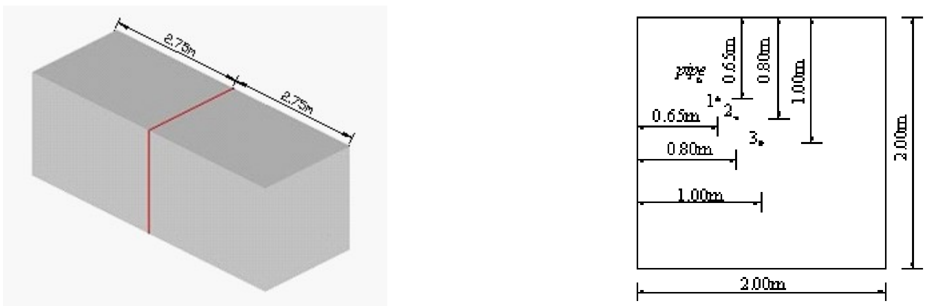

Fig. 23 The position of the typical cross-section points

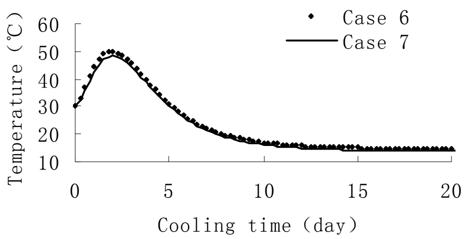

(a) Duration curve of point #1

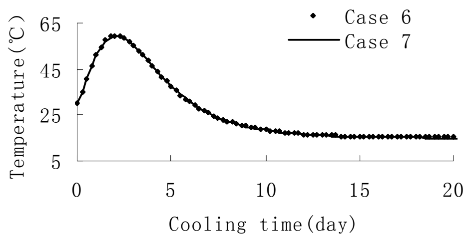

(b) Duration curve of point #2

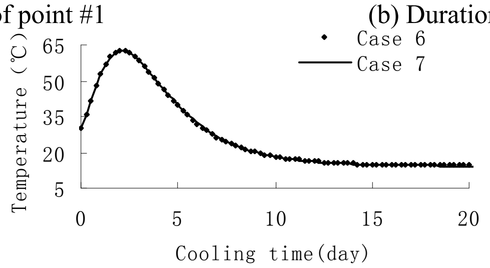

(c) Duration curve of point #3

Fig. 24 Temperature duration curves of typical points

In Fig. 24, the maximum temperature difference between example 1 (using small size element and conventional FEM method) and example 3 is 1.8°C for typical point #1. For the other points, the temperatures of two cases were almost same. However, for the concrete at a certain distance from the pipe, the temperature distribution is almost same for both examples.

Compared with octagonal pipe cross-section, using a square can reduce the number of grid

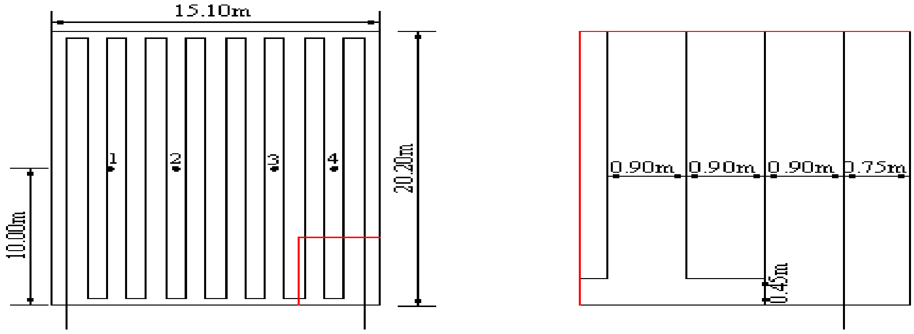

(a) Layout of the pipe (b) Local enlargement

Fig. 25 Layout of the pipe and typical points

points. For structures besides thin walls, the influence range of the pipe cross-section shape is very small, so using a square pipe cross-section is reasonable.

4.4 Numerical example 4

There is an engineering example to demonstrate that this new method is applicable to the actual engineering with snake-shaped water pipes.

4.4.1 Basic information

A bedding cushion of a concrete dam located in the south of China was constructed in September 2009. The height of the bedding cushion is 2.0 m. The pipe was embedded 1.0 m above the foundation. The layout of the pipe is shown in Fig. 25. A steel pipe was used, and the cooling time was 20.0*d*. The cooling water flux is 31.2 m^3/d. The average inlet water temperature is 15.0°C. Under the influence of air temperature, inlet water temperature fluctuates every day. However, with strict temperature control measures, the variation of the inlet water temperature is less than 2.0°C. The placement temperature was about 18°C with little variation under strict placement temperature control measures. The cooling measurement was taken once after placement.

During the cooling time, there was no rain. The average air temperature was 25.5°C with a variation of ±5.0°C. One layer of heat preservation quilt was used after placement, and the heat convection coefficient between the concrete and air was 14.5 kJ/ (m^2 h $^{\circ}$C).

4.4.2 Bedding cushion mesh

Mesh and layout of the pipe are shown in Fig. 26.

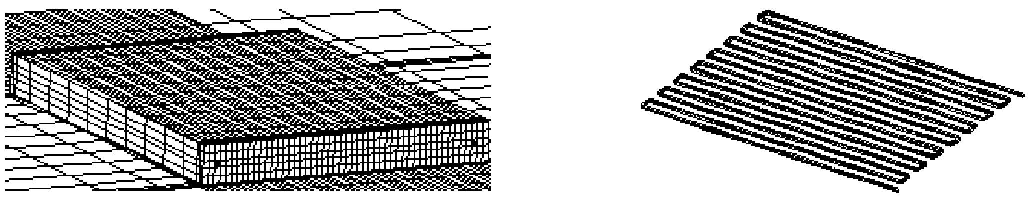

(a) FEM mesh for bedding cushion (b) Layout of the mesh

Fig. 26 Mesh for calculation

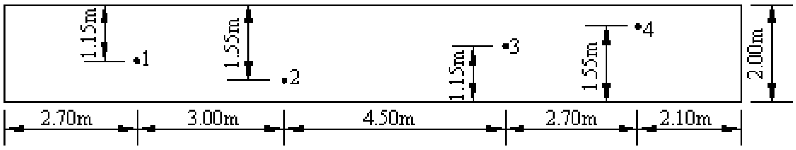

Fig. 27 Front view of typical points

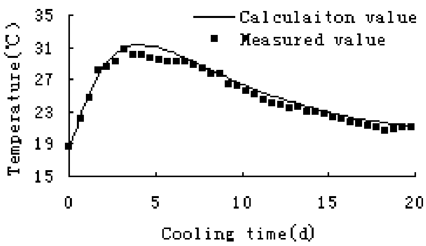

(a) Duration curve of point #1

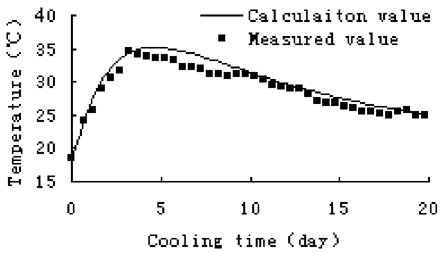

(b) Duration curve of point #2

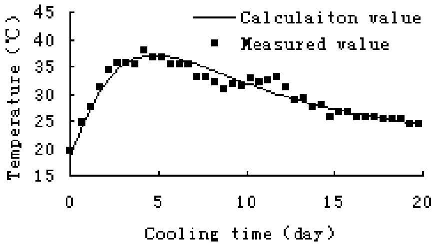

(c) Duration curve of point #3

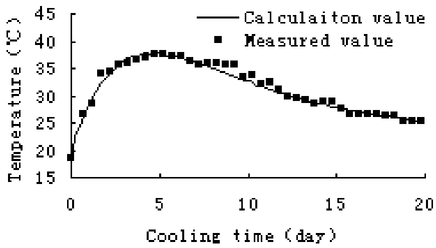

(d) Duration curve of point #4

Fig. 28 Temperature duration curves of typical points

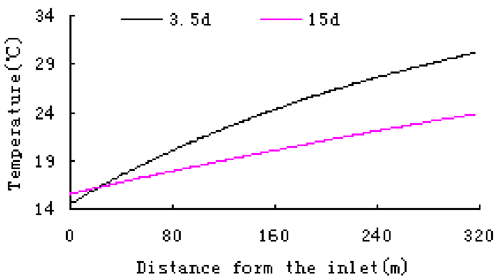

Fig. 29 Water temperature distributions along the pipe

4.4.3 Calculation analysis

Four typical points were chosen for better analysis. The positions of the typical points are shown in Fig. 25(a) and Fig. 27. Fig. 28 is the comparison between the calculation value and the measured value. The value obtained using the proposed method was close to the actual value.

The water temperature distributions along the pipe (3.5 d and 15.0 d after cooling) are shown in Fig. 29. The measured outlet let water temperatures were 31.2°C (3.5*d*) and 22.3°C (15.0*d*). The calculated outlet water temperatures were close to the actual temperatures, which also prove that the new method is reliable.

5. Conclusions

Based on the properties of the temperature gradient around pipes and an explicit iterative algorithm, a new method for solving the temperature field of mass concrete with cooling pipes was proposed. A corresponding 3D finite element program was also developed.

Numerical examples 1 and 2 showed that, compared to conventional FEM, this new method requires much fewer grid points to achieve the same accuracy. From the comparison between the calculated values and actual values in a bedding cushion, the 3D finite element program developed could effectively predict the temperature distribution and history of concrete and water along a pipe.

In conventional computing models, the cooling pipes are regarded as a third boundary condition when solving a model of concrete with plastic pipes. The coefficient of this kind of boundary condition should be got by experiment and inversion, and it is sometimes unreliable. In the proposed method, the function of the pipe is expressed by the heat flux of the concrete around the water pipe, the thermal conductivity, the thickness of the pipe and the temperature of inner surface, which is more reliable and economical.

Acknowledgments

The authors are pleased to acknowledge the financial support for this research by National Natural Science Funds of China (Nos. 51109071, 51209219), Natural Science Funds of Jiangsu Province (No. BK2010517), Fundamental Research Funds for the Central Universities (No.2009B07814), and Priority Academic Program Development of Jiangsu Higher Education Institutions.

References

Deng, J.Q. and Zhu, Y.M. (2008), “Method for grid division of finite elements based on coordinate transformation of super-element shape function and for grid subdivision of cooling water pipe”, *Nature Sci.*, **30**(2), 8-12.

Dundulis, G., Uspuras, E., Kulak, R.F. and Marchertas, A. (2007), “Evaluation of pipe whip impacts on neighboring piping and walls of the Ignalina Nuclear Power Plant”, *Nucl. Eng. Des.*, **237**(8), 848-857.

He, J. and Hoyano, A. (2010), “Experimental study of cooling effects of a passive evaporative cooling wall constructed of porous ceramics with high water soaking-up ability”, *Build. Environ.*, **45**(2), 461-472.

Kawaraba, H., Kanokogi, T. and Tanabe, T. (1986), “Development of the FEM program for the analysis of pipe cooling effects on the thermal stress of massive concrete”, *Trans JCI.*, **8**, 125-130.

Kim, J.K., Kim, K.H. and Yang, J.H. (2001), “Thermal analysis of hydration heat in concrete structures with pipe-cooling system”, *Comput. Struct.*, **79**(2), 163-171.

Koschenz, M. and Dorer, V. (1999), “Interaction of an air system with concrete core conditioning”, *Energy Build.*, **30**(2), 139-145.

Machida, N. and Uehara, K. (1987), “Nonlinear thermal stress analysis of a massive concrete structure”, *Comput. Struct.*, **26**(1-2), 287-296.

De Schutter, G. (2002), “Finite element simulation of thermal cracking in massive hardening concrete elements using degree of hydration based material laws”, *Comput. Struct.*, **80**(27-30), 2035-2042.

Silin, N., Masson, V.P., Osorio, D. and Converti, J. (2010), “Hydrodynamic transition delay in rectangular channels under high heat flux”, *Ann. Nucl. Energy.*, **37**(4), 615-620.

Tan, B.K., Wong, T.N. and Ooi, K.T. (2010), “A study of liquid flow in a flat plate heat pipe under localized heating”, *Int. J. Therm. Sci.*, **49**(1), 99-108.

Wang, Z.H. and Zhu, Y.M. (2008), “Simulation and analysis of temperature field and stress field of sluice pier concrete during construction”, *J. Tianjin Daxue Xuebao (Ziran Kexue yu Gongcheng Jishu Ban)*, **41**(4), 476-481.

Wang, Z.H., Zhu, Y.M. and Li, F. (2008), “Back analysis of concrete thermal parameters and study of feedback based on genetic algorithm”, *J. Wuhan Ligong Daxue Xuebao (Jiaotong Kexue Yu Gongcheng Ban)*, **32**(4), 599-602.

Xie, H.W. and Chen, Y.L. (2005), “Influence of the different pipe cooling scheme on temperature distribution in RCC arch dams”, *Commun. Numer. Meth. En.*, **21**(12), 769-778.

Ni, Y.Q., Zhang, P., Ye, X.W., Lin, K.C. and Liao, W.Y. (2011), “Modeling of temperature distribution in a reinforced concrete supertall structure based on structural health monitoring data”, *Comput. Concrete*, **8**(3), 293-309.

Zhang, Z.M., Song, Z.T. and Huang, H.Y. (2002), “New theory on adiabatic temperature rise and heat conduction equation of concrete”, *J. Hohai Univ.*, **30**(3), 1-6.

Zhu, B.F. (2003), “A method for computing the adiabatic temperature rise of concrete considering the effect of the temperature of concrete”, *J. Hydrol. Eng.*, **81**(2), 69-73.

Zhu, B.F (2003), “The equivalent heat conduction equation of pipe cooling in mass concrete considering influence of external temperature”, *J. Hydraul. Eng.*, (3), 49-54.

Zhu, B.F (2010), “On pipe cooling of concrete dams”, *J. Hydraul. Eng.*, **41**(5), 505-513.

Zhu, Y.M., Xu, Z.Q. and *et al.* (2003), “A calculation method for solving temperature field of mass concrete with cooling pipes”, *J. Yangtze River Sci. Res. Ins.*, **20**(2), 19-22.

CC